

Analysis of the Potential for a Heat Island Effect in Large Solar Farms

Vasilis Fthenakis^{1,2} and Yuanhao Yu¹

¹ Center for Life Cycle Analysis, Department of Earth and Environmental Engineering, Columbia University, New York, NY

² PV Environmental Research Center, Brookhaven National Laboratory, Upton, NY

Abstract — Large-scale solar power plants are being built at a rapid rate, and are setting up to use hundreds of thousands of acres of land surface. The thermal energy flows to the environment related to the operation of such facilities have not, so far, been addressed comprehensively. We are developing rigorous computational fluid dynamics (CFD) simulation capabilities for modeling the air velocity, turbulence, and energy flow fields induced by large solar PV farms to answer questions pertaining to potential impacts of solar farms on local microclimate. Using the CFD codes Ansys CFX and Fluent, we conducted detailed 3-D simulations of a 1 MW section of a solar farm in North America and compared the results with recorded wind and temperature field data from the whole solar farm. Both the field data and the simulations show that the annual average of air temperatures in the center of PV field can reach up to 1.9°C above the ambient temperature, and that this thermal energy completely dissipates to the environment at heights of 5 to 18 m. The data also show a prompt dissipation of thermal energy with distance from the solar farm, with the air temperatures approaching (within 0.3°C) the ambient at about 300 m away of the perimeter of the solar farm. Analysis of 18 months of detailed data showed that in most days, the solar array was completely cooled at night, and, thus, it is unlikely that a heat island effect could occur. Work is in progress to approximate the flow fields in the solar farm with 2-D simulations and detail the temperature and wind profiles of the whole utility scale PV plant and the surrounding region. The results from these simulations can be extrapolated to assess potential local impacts from a number of solar farms reflecting various scenarios of large PV penetration into regional and global grids.

Index Terms – PV, climate change, heat island, fluid dynamics

I. INTRODUCTION

Solar farms in the capacity range of 50MW to 500 MW are being proliferating in North America and other parts of the world and those occupy land in the range from 275 to 4000 acres. The environmental impacts from the installation and operation phases of large solar farms deserve comprehensive research and understanding. Turney and Fthenakis [1] investigated 32 categories of impacts from the life-stages of solar farms and were able to categorize such impacts as either beneficial or neutral, with the exception of the “local climate” effects for which they concluded that research and observation are needed. PV panels convert most of the incident solar radiation into heat and can alter the air-flow and temperature profiles near the panels. Such changes, may subsequently affect the thermal environment of near-by populations of humans and other species. Nemet [2] investigated the effect on

global climate due to albedo change from widespread installation of solar panels and found this to be small compared to benefits from the reduction in greenhouse gas emissions. However, Nemet did not consider local microclimates and his analytical results have not been verified with any field data. Donovan [3] assumed that the albedo of ground-mounted PV panels is similar to that of underlying grassland and, using simple calculations, postulated that the heat island effect from installing PV on grassy land would be negligible. Yutaka [4] investigated the potential for large scale of roof-top PV installations in Tokyo to alter the heat island effect of the city and found this to be negligible if PV systems are installed on black roofs.

In our study we aim in comprehensively addressing the issue by modeling the air and energy flows around a solar farm and comparing those with measured wind and temperature data.

II. FIELD DATA DESCRIPTION AND ANALYSIS

Detailed measurements of temperature, wind speed, wind direction, solar irradiance, relative humidity, and rain fall were recorded at a large solar farm in North America. Fig. 1 shows an aerial photograph of the solar farm and the locations where the field measurements are taken.

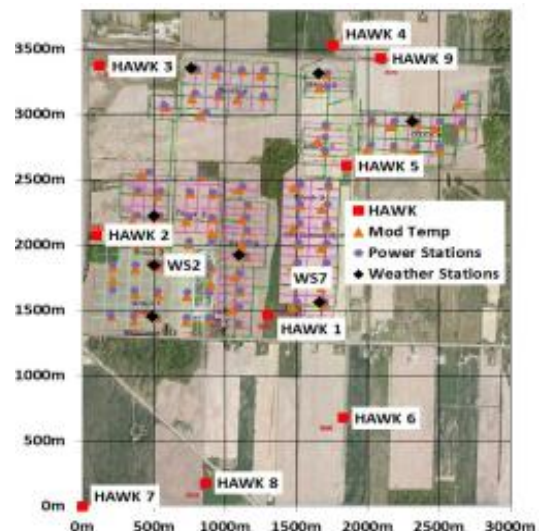


Fig. 1. A picture of the solar farm indicating the locations of the monitoring stations

The field data are obtained from 17 monitoring stations within and around the solar farm, including 8 weather stations (WS) and 9 Hawk stations (HK), all at 2.5 m heights off the ground. There also 80 module temperature (MT) sensors at the back-side of the modules close to each of the corresponding power stations. The WS and MT provide data at 1-min intervals, while the Hawk provides data every 30 minutes. The WS and MT data cover a period of one year from October 2010 to September 2011, while the Hawk data cover a period of 18 months from March 2010 through August 2011.

Hawk stations 3, 6, 7, 8 and 9 are outside the solar farm and were used as reference points indicating ambient conditions. The measurements from Hawk 3, 6, 8 and 9 agree very well confirming that their distances from the perimeter of the solar farm are sufficient for them to be unaffected by the thermal mass of the PV system; Hawk 7 shows higher temperatures likely due to a calibration inaccuracy. In our comparative data analysis we use Hawk 6 as a reference point and, since the prevailing winds are from the south, we selected the section around WS7 as the field for our CFD simulations. Figures 2 to 7 show the difference between the temperatures in Hawk 6 and those in the weather stations WS2 and WS7 within the field, and Hawks 1, 2, 4 and 5 around the solar field.

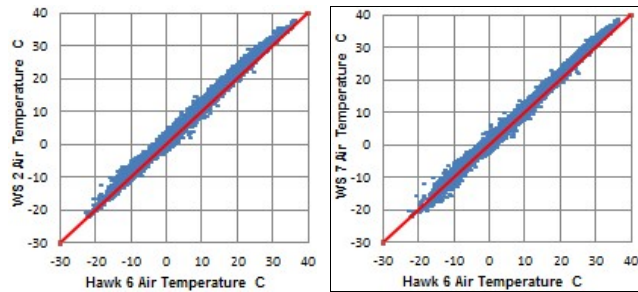


Fig. 2. Air temp WS2 vs. Hawk 6

Fig. 3. Air temp WS7 vs. Hawk6

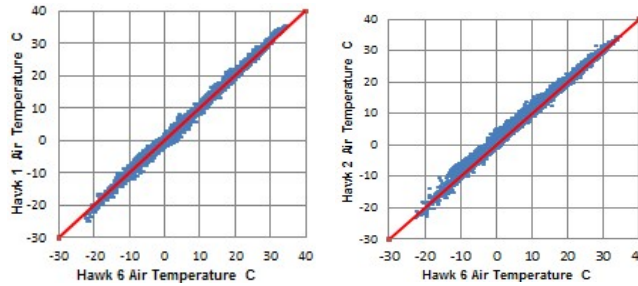


Fig. 4. Air temp Hawk 1 vs. 6

Fig. 5. Air temp Hawk 2 vs. 6

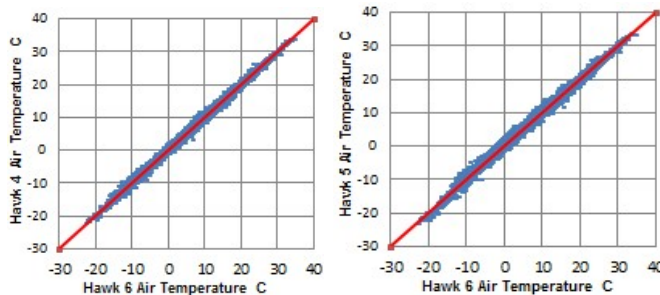


Fig. 6. Air temp Hawk 4 vs. 6

Fig. 7. Air temp Hawk 5 vs. 6

These figures and Table 1 show that with the exception of Hawk 4, the closer the proximity to solar farm the higher the temperature difference from the ambient (indicated by Hawk 6). The relative high temperatures recorded at Hawk 4, and also the relative low temperatures at Hawks 1 and 5 are explained by the prevailing wind direction, which for the time period used in our analysis (8/14/2010-3/14/2011) was Southerly (158°-202°). Hawk 4 is downwind of the solar farm, whereas Hawks 1 and 5 are upwind; the downwind station “feels” more the effect of the heat generated at the solar farm than the ones upwind.

Fig. 8 shows the decline in air temperature as a function of distance to solar farm perimeter. Distances for WS2 and WS7 are negative since they are located inside the solar farm site. WS2 is further into the solar farm and this is reflected in its higher temperature difference than WS7.

TABLE I
DIFFERENCE OF AIR TEMPERATURE (@2.5 M HEIGHTS) BETWEEN THE LISTED WEATHER AND HAWK STATIONS AND THE AMBIENT

Met Station	WS2	WS7	HK1	HK2	HK3	HK4	HK5	HK9
Temp Difference from H6 (°C)	1.878	1.468	0.488	1.292	0.292	0.609	0.664	0.289
Distance to solar farm perimeter (m)	-440	-100	100	10	450	210	20	300

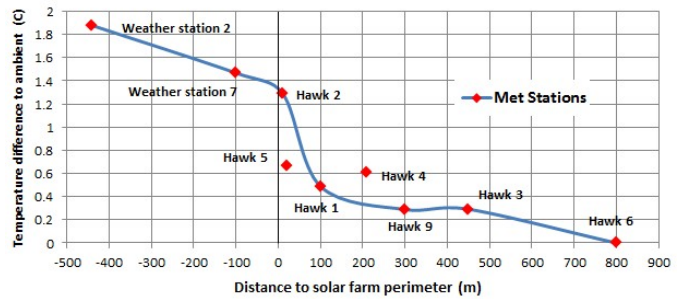


Fig. 8. Air temperature difference as a function of distance from the perimeter of the solar farm. Negative distances indicate locations within the solar farm.

We also examined in detail the temperature differences between the modules and the surrounding air. These vary throughout the year but the module temperatures are consistently higher than those of the surrounding air during the day, whereas at night the modules cool to temperatures below ambient; an example is shown in Fig. 9. Thus, this PV solar farm did not induce a day-after-day increase in ambient temperature, and therefore, adverse micro-climate changes from a potential PV plant are not a concern.

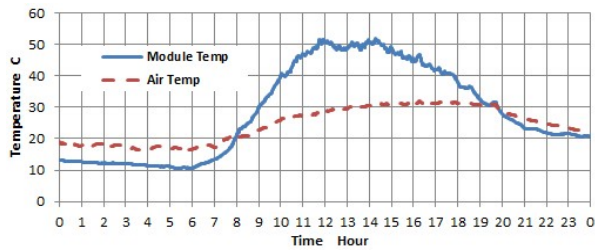


Fig. 9. Comparison of module temperature and air temperature 2.5 m off the ground on a sunny day (July 1, 2011)

III. CFD MODEL DEVELOPMENT

In preliminary simulations we tested the Ansys CFX and FLUENT computational fluid dynamics codes (CFD) and decided to use FLUENT in detailed simulations. FLUENT offers several turbulence schemes including multiple variations of the $k-\epsilon$ models, as well as $k-\omega$ models, and Reynolds stress turbulence models. We used the standard, renormalized-group (RNG), and realizable $k-\epsilon$ turbulence closure scheme as it is the most commonly used model in street canyon flow and thermal stratification studies [5]. FLUENT incorporates the P-1 radiation model which affords detailed radiation transfer between the solar arrays, the ground and the ambient air; it also incorporates standard free convection and wind-forced convection models. Our choice of solver was the pressure-based algorithm SIMPLE which uses a relationship between velocity and pressure corrections to enforce mass conservation and obtain the pressure field. We conducted both three-dimensional (3-D) and 2-D simulations.

A 3-D model was built of four fields each covering an area of 93-meters by 73-meters (Fig. 10). Each field contains 23 linear arrays of 73-meter length and 1.8-meter width. Each array has 180 modules of 10.5% rated efficiency, placed facing south at a 25-degree angle from horizontal, with their bottom raised 0.5 m from the ground and their top reaching a height of 1.3 m. Each array was modeled as a single 73 m \times 1.8 m \times 1 cm rectangular. The arrays are spaced 4 meters apart and the roads between the fields are 8 m. Fig. 10 shows the simulated temperatures on the arrays at 14:00 pm on 7/1/2011, when the irradiance was 966 W/m². As shown, the highest average temperatures occur on the last array (array 46). Temperature on the front edge (array 1) is lower than in the center (array 23). Also, temperature on array 24 is lower than array 23, which is apparently caused by the cooling induced by the road space between two fields, and the magnitude of the temperature difference between arrays 24 and 46 is lower than that between arrays 1 and 23, as higher temperature differences from the ambient, result in more efficient cooling.

TABLE II
MODULES TEMPERATURE

Arrays	1	23	24	46
Temperature °C	46.1	56.4	53.1	57.8

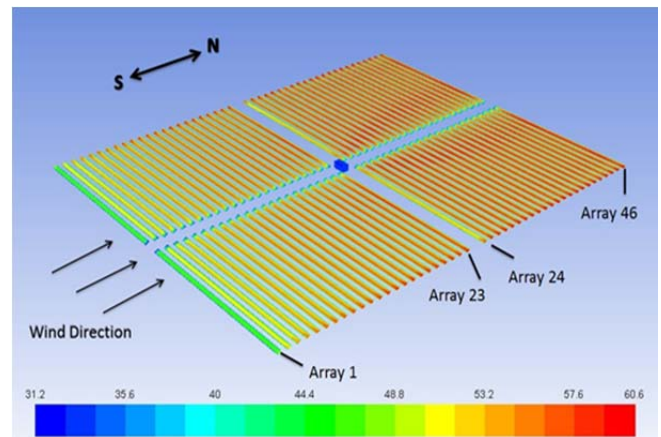
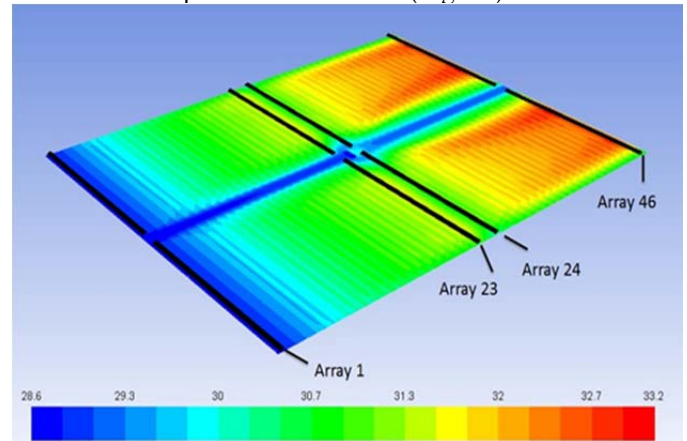
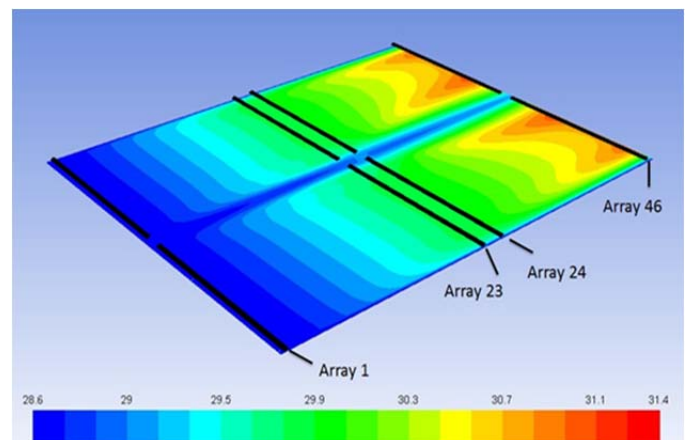


Fig. 10. Module temperatures from 3-D simulations of air flows and thermal exchange during a sunny day

Our simulations also showed that the air temperatures above the arrays at a height of 2.5 m ranged from 28.6 °C to 31.1 °C; the ambient temperature was 28.6 °C (Fig. 11).



(a)



(b)

Fig. 11 Air temperatures from 3-D simulations during a sunny day. a) Air temperatures at a height of 1.5 m; b) air temperatures at a height of 2.5 m.

TABLE III
AIR TEMPERATURE

Temperature	Ambient (°C)	Low (°C)	High (°C)	Average (°C)
2.5m height	28.6	28.6	31.1	30.1
1.5m height	28.6	28.6	33.2	30.8

These simulations show a profound cooling effect with increasing height from the ground. It is shown that the temperatures on the back surface of solar panels is up to 30° C warmer than the ambient temperature, but the air above the arrays is only up to 2.5°C higher than the ambient (i.e., 31.1°C). Also the road between the fields allows for cooling, which is more evident at the temperatures 1.5 m off the ground (Fig. 11a). The simulations show that heat build-up at the power station in the middle of the fields has a negligible effect on the temperature flow fields; it was estimated that a power station adds only about 0.4% to the heat generated by the corresponding modules.

The 3-D model showed that the temperature and air velocity fields within each field of the solar farm were symmetrical along the cross-wind axis; therefore a 2-D model of the downwind and the vertical dimensions was deemed to be sufficiently accurate. A 2-D model reduced the computational requirements and allowed for running simulations for several subsequent days using actual 30-min solar irradiance and wind input data. We tested the numerical results for three layers of different mesh sizes and determined that the following mesh sizes retain sufficient detail for an accurate representation of the field data: a) Top layer: 2m by 1m, b) Middle layer: 1.5m by 0.6m, c) Bottom layer: 1m by 0.4m. According to these mesh specifications, a simulation of 92 arrays (length of 388m, height 9m), required a total of 13600 cells. Figures 12-15 show comparisons of the modeled and measured module and air temperatures.

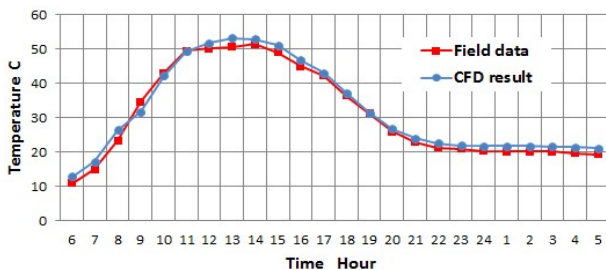


Fig. 12. Comparisons of field and modeled module temperatures; a sunny summer day (7/1/2011); 2-D simulations.

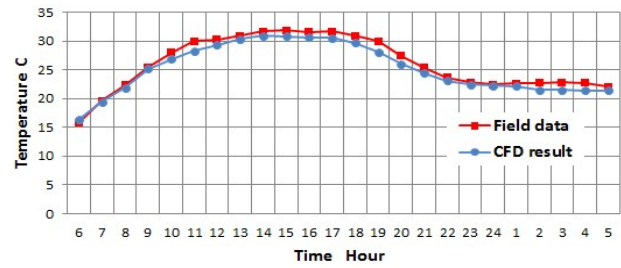


Fig. 13. Comparisons of field and modeled air temperatures at a height of 2.5 m; a sunny summer day (7/1/2011); 2-D simulations.

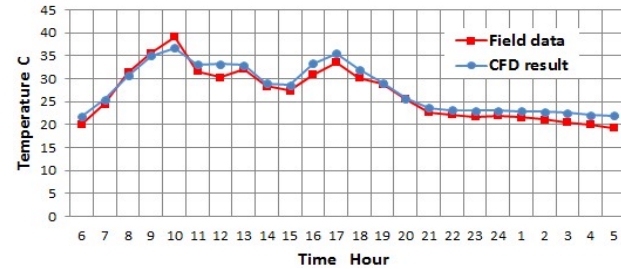


Fig. 14. Comparisons of field and modeled module temperatures; a cloudy summer day (7/11/2011); 2-D simulations.

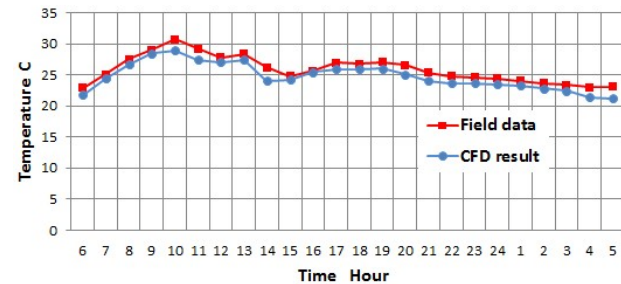
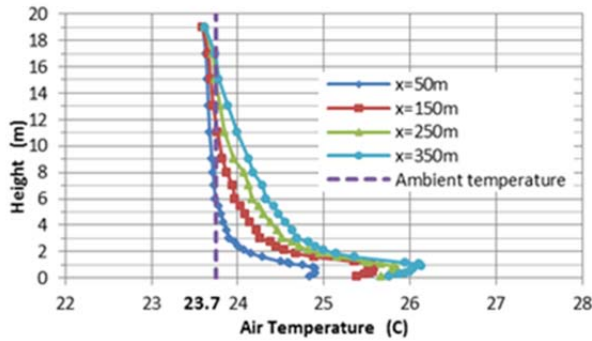
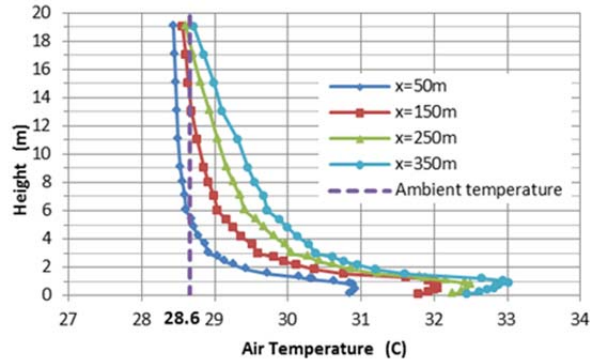


Fig. 15. Comparisons of field and modeled air temperatures at a height of 2.5 m; a cloudy summer day (7/11/2011); 2-D simulations.

Figures 16a and 16b show the air temperature as a function of height at different downwind distances in the morning and afternoon during a sunny summer day. At 9 am (irradiance 500 W/m², wind speed 1.6 m/s, inlet ambient temperature 23.7°C), the heat from the solar array is dissipated at heights of 5-15m, whereas at 2 pm (irradiance 966 W/m², wind speed 2.8m/s, inlet ambient temperature 28.6°C, the temperature of the panels has reached the daily peak, and the thermal energy takes up to 18 m to dissipate.



(a) 9:00 am



(b) 2:00 pm

Fig. 16 Air temperatures within the solar farm, as a function of height at different downwind distances. From 2-D simulations during a sunny summer day (7/1/2011) at 9 am and 2 pm.

IV. CONCLUSION

The field data and our simulations show that the annual average of air temperatures at 2.5 m of the ground in the center of simulated solar farm section is 1.9°C higher than the

ambient and that it declines to the ambient temperature at 5 to 18 m heights. The field data also show a clear decline of air temperatures as a function of distance from the perimeter of the solar farm, with the temperatures approaching the ambient temperature (within 0.3°C), at about 300 m away. Analysis of 18 months of detailed data showed that in most days, the solar array was completely cooled at night, and, thus, it is unlikely that a heat island effect could occur.

Our simulations also show that the access roads between solar fields allow for substantial cooling, and therefore, increase of the size of the solar farm may not affect the temperature of the surroundings. Simulations of large (e.g., 1 million m²) solar fields are needed to test this hypothesis.

ACKNOWLEDGEMENT

We are grateful to First Solar for providing data for this study.

REFERENCES

- [1] D. Turney and V. Fthenakis Environmental, "Impacts from the installation and operation of large-scale solar power plants," *Renewable and Sustainable Energy Reviews*, vol. 15, pp. 3261-3270, 2011.
- [2] F.G. Nemet. "Net radiative forcing from widespread deployment of photovoltaics," *Environ. Sci. Technol.*, vol. 43, pp. 2173-2178, 2009.
- [3] M. Donovan, "Memorandum: impact of PV systems on local temperature," *SunPower*, July 6, 2010. http://www.rurdev.usda.gov/SupportDocuments/EA_5_17_13_RUS_PartA.pdf
- [4] Y. Genchi, M. Ishisaki, Y. Ohashi, H. Takahashi, & A. Inaba, "Impacts of large-scale photovoltaic panel installation on the heat island effect in Tokyo," in *Fifth Conference on the Urban Climate*, 2003.
- [5] Theory Guide, *ANSYS Fluent HELP 13*.